sustainability

MDPI

Article

Optimal Feeder Reconfiguration and Placement of Voltage Regulators in Electrical Distribution Networks Using a Linear Mathematical Model

Luis A. Gallego Pareja [1], Jesús M. López-Lezama [2,*] and Oscar Gómez Carmona [3]

[1] Department of Electrical Engineering, State University of Londrina (UEL), Londrina 86057-970, PR, Brazil
[2] Research Group in Efficient Energy Management (GIMEL), Departamento de Ingeniería Eléctrica, Universidad de Antioquia, Calle 67 No. 53-108, Medellín 050010, Colombia
[3] Facultad de Tecnología, Universidad Tecnológica de Pereira, Cr 27 No 10-02, Pereira 660003, Colombia
* Correspondence: jmaria.lopez@udea.edu.co

Abstract: Power distribution systems face continuous challenges from increased demand and lengthening of feeders, resulting in power loss augmentation and unacceptable voltage drops. Thus, to reduce technical losses and improve the voltage profile, common techniques such as reactive compensation, network reconfiguration, and placing of voltage regulators are employed. Distribution network reconfiguration (DNR) consists of modifying the system topology with the aim of minimizing power losses, enhancing voltage profile, and improving network reliability. Optimal placement of voltage regulators (OPVRs) improves the voltage profile and helps to reduce power losses. DNR and OPVRs are challenging optimization problems involving both integer and continuous decision variables. In this paper, a mixed-integer linear programming (MILP) model is presented to simultaneously solve the problems of DNR and OPVRs in radial distribution networks. The combined optimal DNR and OPVRs aim at both the minimization of power losses and the improvement of the voltage profile. This approach has not been reported in the specialized literature. The proposed MILP model may be solved through commercially available software, obtaining global optimal solutions with lower computational effort than metaheuristic techniques applied for the same purpose. Several tests were conducted on three benchmark distribution test systems to demonstrate the efficacy and applicability of the proposed approach.

Keywords: distribution network; mixed-integer linear programming; reconfiguration; voltage regulators

Citation: Gallego Pareja, L.A.; López-Lezama, J.M.; Gómez Carmona, O. Optimal Feeder Reconfiguration and Placement of Voltage Regulators in Electrical Distribution Networks Using a Linear Mathematical Model. *Sustainability* **2023**, *15*, 854. https://doi.org/10.3390/su15010854

Academic Editor: Mohamed A. Mohamed

Received: 18 October 2022
Revised: 1 December 2022
Accepted: 30 December 2022
Published: 3 January 2023

1. Introduction

Power distribution systems (PDS) are composed of main feeders and laterals and constitute the link between the sub-transmission power system and the consumers. The primary feeders originate from the substation and pass through the main load centers, and they have lateral distributors to connect the individual load points. These systems are well known for their high resistance vs. inductive reactance ratio and significant voltage drop, so one of the most important tasks in large distribution systems is to keep the voltage profiles under control [1]. The most common strategies adopted in distribution planning for the reduction of power losses and voltage profile improvement include feeder reconfiguration, reinforcement of feeders, construction of new substations, reactive power compensation, and installing voltage regulators, among others. This paper focuses on distribution network reconfiguration (DNR) and the optimal placement of voltage regulators (OPVRs) from the standpoint of distribution planning.

DNR consists of finding a new topology for the system to minimize power losses, ameliorate the voltage profile, and enhance network reliability. DNR is carried out by altering the states of sectionalizing and tie switches, which are normally open or closed, respectively [2,3]. Nonetheless, in radial distribution networks with heavily loaded feeders

and a poor voltage profile, DNR may not be enough to ameliorate the voltage profile, and VRs may be a suitable option. From the standpoint of mathematical optimization, DNR is a mixed integer nonlinear (MINL) optimization problem whose solution is a challenging task due to the high number of possible network topologies that result from the combination of each switch status. This problem must consider a set of constraints that involve not only limits on electrical magnitudes but also those regarding its topology (candidate solutions must remain radial). Due to the nature of the DNR problem, a bunch of metaheuristic optimization techniques have been applied to its solution. Metaheuristic techniques have been commonly inspired by natural phenomena, as well as biological and physical processes. In electrical engineering, metaheuristics approaches have been extensively used to tackle nonlinear and non-convex optimization problems [4–9].

Genetic algorithms (GAs) are inspired by the process of natural selection. Every solution candidate is represented by a chromosome or vector that contains the decision variables of the optimization problem [10]. Several variants and hybrid approaches of GA have been used to solve the DNR problem. In [11], the authors propose a nondominated sorting genetic algorithm to solve the multiobjective DNRP considering the minimization of real power losses, improvement of voltage profile, and load balancing. The proposed GA provides a set of possible solutions over which the system planner must decide. In [12], a GA inspired by graph theory is developed. In this case, tie branches are obtained by a spanning tree, and each spanning tree is associated with a subpopulation of the GA. The main advantage of this approach is that unfeasible solutions are not generated in the reconfiguration stage of the GA.

Harmony Search (HS) is a relatively new metaheuristic that is inspired by the improvisation process of musicians when trying to find a pleasing harmony. The authors in [13] implement an HS algorithm to solve the reconfiguration problem, aiming at minimizing power losses. In [14], the authors proposed an enhanced version of HS applied to the DNR problem that allows the detection of islands, facilitating the enforcement of the radiality constraint. In [15], the authors combined HS with path relinking to reduce the computational cost of the DNR process, accelerating the convergence of the metaheuristic.

Particle Swarm Optimization (PSO) was inspired by the behavior of organisms within a bird flock or fish school. In PSO, each candidate solution is represented as a particle whose position and velocity are updated in each iteration considering the local and global best-known positions. In [16–18], PSO is applied to solve the optimal DNR problem. In [16], the DNR is solved for the minimization of power losses and improvement of the voltage profile. In [17], the optimal DNR is developed based on a multiobjective function. The objectives include the minimization of active and reactive power losses, the minimization of voltage deviations, and the improvement of system reliability. As evidenced in the literature review, the DNR is a widely studied subject. A review regarding a classification of different techniques applied to solve this problem can be consulted in [19].

A voltage regulator (VR) is essentially an auto-transformer consisting of a primary winding connected in parallel with the circuit and a secondary winding with automatic taps connected in series with the circuit. They are mainly used in large and loaded feeders where reactive compensation or network reconfiguration does not have a sufficient effect. When a VR is installed at a node, it improves the voltage at the nodes beyond the location of the VR. The increase in voltage successively causes a reduction in losses in the system. The use of VRs is constrained due to their elevated investment costs, so the optimal location of these devices becomes an important issue. VRs pose two problems that must be addressed. The first one is to determine the number of necessary VRs and their locations on the network, while the second one concerns the selection of their tap positions. The optimal placement and setting of VRs have a discrete and combinatorial nature, so their complexity will increase exponentially with the number of possibilities. The optimal placement of VRs (OPVRs) is not a new topic for researchers; several papers have addressed this problem in PDS with different approaches.

A sequential algorithm that places VRs by sweeping the network from the source to the ends is proposed in [20]; then, it uses a recursive procedure to examine whether fewer VRs contribute an acceptable voltage profile to the network while simultaneously reducing the value of investment and maintenance cost. The authors in [21] propose power loss indices for an initial selection of VR buses; then, Particle Swarm Optimization (PSO) is used for optimal location, number, and tap setting of VRs. In [22], the authors calculate voltage drops at each branch to select the best location for VRs; then, a GA is used to find the best selection of their tap positions. In [23], the OPVR in PDS is carried out using a two-step algorithm. Initially, several VRs are placed in candidate buses with given tap positions; then, an attempt is made to reduce the number of VRs, taking into consideration economic aspects. In [24], the authors propose two methods for selecting the optimal number, location, and tap settings of VRs in PDS; the first is an analytical method, while the second one consists of a fuzzy expert system containing a set of heuristic rules.

The authors in [25] implement a Plant Growth Simulation Algorithm (PGSA) for OPVRs in PDS. In [26], a GA is used to optimize an objective function that considers losses and voltage drop indices. Further, multiple hourly deterministic optimization processes are applied, considering the daily load profiles of each node. In [27], the authors made the selection of voltage regulator nodes through a power loss index; then, a discrete PSO was used to determine the tap setting of the VRs. In [28], the authors propose back-tracking algorithms and fuzzy logic for OPVRs. In [29], two optimization methods were implemented for OPVRs: a GA and a modified Tabu Search (TS) algorithm. The GA finds candidate regions where the solution may be, while the TS provides a local search in the regions defined by the GA. In [30], the authors use a GA to determine the number, location, and rated power of VRs, while tap positions are achieved through local controllers. Power loss indices and an Artificial Bee Colony (ABC) algorithm are used in [31] to determine the number, location, and tap positions of VRs in PDS. As can be seen, many techniques based on sequential algorithms, stochastic search, and hybrid versions have been used to solve the optimal placement and tap setting of VRs in PDS. Nonetheless, a common drawback of these approaches is the probability of getting trapped in locally optimal solutions. Furthermore, the computation time can be prohibitive for large distribution systems.

VRs help to improve the voltage profile but have little impact on reducing power losses. This is because these devices do not inject power into the network. In fact, OPVRs are often combined with other methods to reduce power losses and improve the voltage profile. In [32], the authors use a fuzzy logic optimization method for the location of VR and CBs. Voltages and power loss indices were modeled using fuzzy membership functions, and a fuzzy expert system containing a set of heuristic rules was used to determine VRs and CBs placement. In the same way, VR locations were combined with the locations of CBs and Distributed Generators (DGs) jointly. In [33], an Enhanced Grey Wolf Algorithm is presented for solving the coordinated allocation of CBs, DGs, and VRs. The authors in [34] proposed a mixed integer nonlinear programming problem, which is solved by employing a specialized GA to optimize the location of CBs, DGs, and VRs all together, in pairs, or separately.

As was evident in the literature review, several optimization techniques have been applied to solve both the optimal DNR and OPVRs. Nonetheless, to the best of the author's knowledge, the combined optimal DNR and OPVRs have not been approached in the specialized literature. Nonetheless, it constitutes an adequate option for minimizing power losses and improving the voltage profile. Furthermore, few studies have used linearized models for DNR or OPVRs. In this sense, the main contributions of this paper are threefold: (1) A MILP model is proposed to solve the simultaneous DNR and OPVRs in PDS, a problem that has not been previously addressed in the specialized literature; (2) due to its nature, the proposed approach is able to find globally optimal solutions instead of locally optimal solutions; and (3) the proposed model can be implemented and solved through commercially available solvers and it can be applied to real-size distribution networks.

Three distribution test systems of 33, 69, and 119 buses were used to validate the proposed approach. As regards the optimal DNR alone for the 33 and 69-bus test systems, the proposed approach was able to replicate the same results reported in the specialized literature. Furthermore, as simultaneous DNR and OPVRs have not been reported in the specialized literature, this paper may serve as a reference for future work in this area.

The rest of this document is organized as follows: Section 2 presents a nonlinear power flow model that is linearized before introducing constraints for both DNR and VRs. Next, a linear model is presented for the simultaneous optimal DNR and OPVRs in PDS. The results are presented with three benchmark distribution test systems for optimal DNR, OPVRs independently, and both problems combined in Section 3. Section 4 compares the results with works involving either reconfiguration or optimal placement of voltage regulators; finally, Section 5 presents the research's conclusions.

2. Mathematical Model

This section presents the proposed MILP model to solve the DNR problem along with OPVRs. In this case, both problems can be solved either separately or together. The daily operation of modern EDNs that require reconfiguration poses important challenges to engineers, such as temporarily meshed operations, network disturbances, temporary interruptions, and even problems with the protection coordination scheme that must be recalculated according to the new topology [35,36]. In this sense, it is worth mentioning that the proposed approach relates to the planning problem of the EDN rather than its daily operation. The proposed model allows the optimal number and settings of VRs in a distribution network that can adapt its topology through reconfiguration to minimize power losses to be found while keeping the system variables within specified limits.

2.1. Nonlinear Power Flow for Radial Distribution Networks

The nonlinear load flow for radial EDNs is described by Equations (1)–(7) [3,37,38]. The system is represented by its monophasic equivalent, the capacitive effect of distribution lines is neglected, and only one source is considered (the substation). The objective function, introduced by Equation (1), consists of minimizing the cost of active power losses. In this case, k_c denotes the interest rate associated with the active power losses cost, Ω_l denotes the set of branches, while I_{ij} and R_{ij} are the current and resistance of branch ij, respectively.

$$\text{Minimize } v = k_c \sum_{\forall ij \in \Omega_l} R_{ij} \cdot I_{ij}^2 \tag{1}$$

Subject to:

$$\sum_{\forall ki \in \Omega_l} P_{ki} - \sum_{\forall ij \in \Omega_l} \left(P_{ij} + R_{ij} I_{ij}^2 \right) + P_i^s = P_i^d;\ \forall i \in \Omega_b \tag{2}$$

$$\sum_{\forall ki \in \Omega_l} Q_{ki} - \sum_{\forall ij \in \Omega_l} \left(Q_{ij} + X_{ij} I_{ij}^2 \right) + Q_i^s = Q_i^d;\ \forall i \in \Omega_b \tag{3}$$

$$V_i^2 - 2\left(R_{ij} P_{ij} + X_{ij} Q_{ij} \right) - Z_{ij}^2 I_{ij}^2 - V_j^2 = 0;\ \forall ij \in \Omega_l \tag{4}$$

$$V_j^2 I_{ij}^2 = P_{ij}^2 + Q_{ij}^2;\ \forall\, ij \in \Omega_l \tag{5}$$

$$0 \le I_{ij} \le \overline{I}_{ij};\ \forall\, ij \in \Omega_l \tag{6}$$

$$\underline{V}_i \le V_i \le \overline{V}_i;\ \forall i \in \Omega_b \tag{7}$$

The balance of active and reactive power for every bus of the system is described by Equations (2) and (3), respectively. In this case, P_{ki} and P_{ij} represent the active power flow in lines ki and ij, while Q_{ki} and Q_{ij} stand for the reactive power flow in lines ki and ij, respectively. P_i^s and Q_i^s represent, respectively, the active and reactive power provided by the substation at node i. P_i^d and Q_i^d are the active and reactive power demands at bus i (kW,

kVAr). R_{ij} and X_{ij} are the resistance and reactance of branch ij (kΩ), respectively. Finally, Ω_l is the set of buses.

The constraint given by Equation (4) models the voltage drop in every line ij. Voltage magnitudes are computed in terms of the power flow through the line and its electrical parameters. In [39], it is proposed to eliminate the voltage angle, obtaining Equation (4), where Z_{ij} represents the impedance of line ij, while V_i is the voltage at bus i. Equation (5) is the apparent power, which is equal to the square of the voltage, j, times the square of the current ij. Constraints (6) and (7) represent the limits of the current through branch ij and the voltage at bus i, respectively. In this case, $\overline{V}_i$ and $\underline{V}_i$ represent the upper and lower voltage limits at bus i, while $\overline{I}_{ij}$ is the upper current limit of branch ij. Note that the lower current limit is considered zero. The power flow given by Equations (1)–(7) is nonlinear. Note that the voltage and currents in this model are squared. Therefore, as proposed in [37,38], a change in variables can be carried out to reduce the nonlinearity of the model. In this case, V_i^2, V_j^2, and I_{ij}^2 can be replaced by a new set of variables labeled as V_i^{sqr}, V_j^{sqr}, and I_{ij}^{sqr}. This change in variables is applied in the model from here on.

2.2. Objective Function

The objective function that minimizes the power losses and investment cost through the optimal DNR and OPVRs is given by Equation (8).

$$\text{Minimize } v = k_e \sum_{\forall ij \in \Omega_l} R_{ij} \cdot I_{ij}^{sqr} + D \cdot C^{vr} \sum_{\forall ij \in \Omega_l} W_{ij}^{vr} \tag{8}$$

In this case, D represents a factor of depreciation applied to the installation of VRs, C^{vr} is the cost of VR purchase and installation, and W_{ij}^{vr} is a binary variable that indicates whether a VR is placed on line ij.

2.3. Constraints Related to the OPVRs and DNR

A voltage regulator can be defined as an autotransformer that features an automatic changing mechanism of the tap position. This device maintains a voltage magnitude at a predetermined value despite load variations. VRs have a reversing switch, enabling a ±R% regulator range (usually 10%). The maximum number of steps is usually 33 (16 steps to increase the voltage magnitude, 16 steps to decrease it, plus the neutral position). Figure 1 depicts a voltage regulator located in branch ij to control the voltage of bus j. In this case, the non-regulated voltage is $\widetilde{V}_j$, the regulated voltage is V_j, and t_{ij} is the voltage regulator tap.

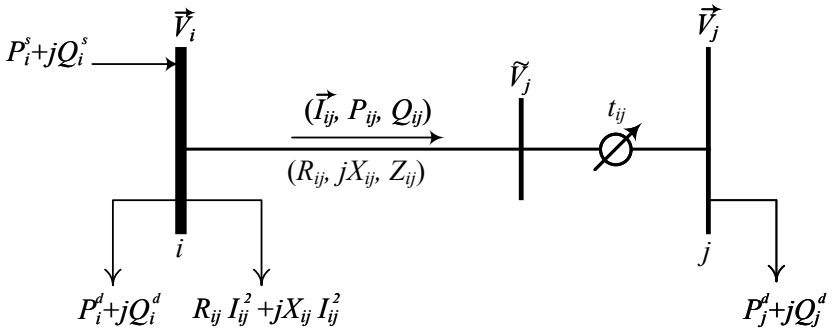

Figure 1. Voltage Regulator.

Equations (9)–(12) present the mathematical model of the voltage regulator located in branch ij.

$$V_j = t_{ij} \cdot \widetilde{V}_j;\ \forall ij \in \Omega_l \tag{9}$$

$$t_{ij} = 1 + \left(\frac{R\%}{\overline{N}^{vr}}\right) \cdot nt_{ij};\ \forall ij \in \Omega_l \tag{10}$$

$$-\overline{N}^{vr} \leq nt_{ij} \leq \overline{N}^{vr};\ \forall ij \in \Omega_l \tag{11}$$

$$nt_{ij};\ \text{integer};\ \forall ij \in \Omega_l \tag{12}$$

In this case, $\overline{N}^{vr}$ represents the number of steps of the VR. nt_{ij} is the voltage regulator tap, nt_{ij} is the integer variable that indicates the tap position.

The voltage profile in the system branches can be computed through Equation (4), which can be rewritten as in Equation (13) to consider the optimal DNR and OPVRs:

$$V_i^{sqr} - 2(R_{ij}P_{ij} + X_{ij}Q_{ij}) - Z_{ij}^2 I_{ij}^{sqr} - \widetilde{V}_j^{sqr} - b_{ij} = 0; \quad \forall ij \in \Omega_l \tag{13}$$

where b_{ij} is an auxiliary variable that enforces Equation (13).

According to [37], the apparent power in branch ij, given by Equation (5), is modified as follows to consider the OPVRs:

$$\widetilde{V}_j^{sqr} \cdot I_{ij}^{sqr} = P_{ij}^2 + Q_{ij}^2;\ \forall ij \in \Omega_l \tag{14}$$

Equations (6) and (7) are modified as shown in (15) and (16).

$$0 \leq I_{ij}^{sqr} \leq \overline{I}_{ij}^2\ \forall ij \in \Omega_l \tag{15}$$

$$\underline{V}_i^2 \leq V_i^{sqr} \leq \overline{V}_i^2;\ \forall i \in \Omega_b \tag{16}$$

Equations (17)–(24) are used to represent the DNR problem. According to Equation (17), the current limit in branches represented by Equation (15) is modified.

$$0 \leq I_{ij}^{sqr} \leq \overline{I}_{ij}^2\left(y_{ij}^+ + y_{ij}^-\right); \forall ij \in \Omega_l \tag{17}$$

$$0 \leq P_{ij}^+ \leq \overline{V}\ \overline{I}\ y_{ij}^+; \forall ij \in \Omega_l; \forall ij \in \Omega_l \tag{18}$$

$$0 \leq P_{ij}^- \leq \overline{V}\ \overline{I}\ y_{ij}^-; \forall ij \in \Omega_l; \forall ij \in \Omega_l \tag{19}$$

$$|Q_{ij}| \leq \overline{V}\ \overline{I}\left(y_{ij}^+ + y_{ij}^-\right); \forall ij \in \Omega_l \tag{20}$$

$$|b_{ij}| \leq \left(\overline{V}^2 - \underline{V}^2\right)\left(1 - \left(y_{ij}^+ + y_{ij}^-\right)\right); \forall ij \in \Omega_l \tag{21}$$

$$\sum_{ij \in \Omega_l}\left(y_{ij}^+ + y_{ij}^-\right) = N - 1; \forall ij \in \Omega_l \tag{22}$$

$$\left(y_{ij}^+ + y_{ij}^-\right) \leq 1; \forall ij \in \Omega_l \tag{23}$$

$$y_{ij}^+;\ y_{ij}^-;\ \ binary; \forall ij \in \Omega_l \tag{24}$$

where b_{ij} is zero if circuit ij is closed, as indicated by Equation (21); otherwise, b_{ij} may take any value limited by Equation (22) to account for Equation (23); y_{ij}^+ and y_{ij}^- represent binary variables related to the power flow direction of branch ij. If any one of the variables equals one, the switch in this branch is closed; if both variables are zero, the circuit is open. Finally, N is the number of buses.

The current limit is represented by constraint (17), which is a function of the variables y_{ij}^+ and y_{ij}^-. The limit of variables P_{ij}^+ and P_{ij}^- are represented by constraints (18) and (19). The reactive power flow limit in branch ij is represented by constraint (20). Constraint (21) represents the limit of b_{ij}. The EDN is guaranteed to be radial by constraint (22). Variables y_{ij}^+ and y_{ij}^- are binary according to constraint (24).

2.4. Linearization of the Mathematical Model

This section presents the linearization process of the power flow and the mathematical model of voltage regulators. The model for the DNR problem is linear, so it does not have to be linearized. The validation of the linear power flow is presented in detail in [40], where it is tested with seven different distribution systems ranging from 33 to 417 buses. When compared with the traditional nonlinear approach, the relative error regarding power losses ranges from 0.0099% to 0.1870%, which shows the accuracy of the linearization approach.

Initially, the left-hand side of Equation (14) is linearized, as indicated by Equations (25)–(30) [37].

$$\widetilde{V}_j^{sqr} I_{ij}^{sqr} = \left(\underline{V}^2 + \frac{1}{2}\Delta V\right) I_{ij}^{sqr} + \sum_{s=1}^{S} P_{j,s}^{c};\ \ \forall ij \in \Omega_l \tag{25}$$

$$\underline{V}^2 + \sum_{s=1}^{S}\left(\Delta V \cdot x_{j,s}\right) \le \widetilde{V}_j^{sqr} \le \underline{V}^2 + \sum_{s=1}^{S}\left(\Delta V \cdot x_{j,s}\right) + \Delta V;\ \ \forall j \in \Omega_b \tag{26}$$

$$x_{j,s} \le x_{j,s-1};\ \ \forall j \in \Omega_b; s = 2..S \tag{27}$$

$$x_{j,s} \in \{0,1\};\ \ \forall j \in \Omega_b; s = 1..S \tag{28}$$

$$0 \le \Delta V \cdot I_{ij}^{sqr} - P_{j,s}^{c} \le \Delta V \cdot \overline{I}_{ij}^{2}\left(1 - x_{j,s}\right); \forall ij \in \Omega_l, s = 1..S \tag{29}$$

$$0 \le P_{j,s}^{c} \le \Delta V \cdot \overline{I}_{ij}^{2}\, x_{j,s};\ \forall ij \in \Omega_l \tag{30}$$

where ΔV is the discretization step, S is the number of discretizations, $P_{j,s}^{c}$ is the power correction used in $\widetilde{V}_j^{sqr} \cdot I_{ij}^{sqr}$, and $x_{j,s}$ is a binary variable used in the discretization of $\widetilde{V}_j^{sqr}$.

Constraint (25) results in using the middle point of the first interval of the discretization of the square voltage magnitude multiplied by the square current flow magnitude plus the successive power corrections ($P_{j,s}^{c}$). It is a linear approximation of $\widetilde{V}_j^{sqr} I_{ij}^{sqr}$. Constraint (26) specifies the range of possible values for voltage ($\widetilde{V}_j^{sqr}$) in the proposed linearization. Constraint (27) states that the binary variable $x_{j,s-1}$ must be greater than variable x_j, s. Constraint (28) indicates the nature of the variable implemented in the linearization scheme (binary variable). The values of P_j, sc are defined by constraints (29) and (30). If $x_{j,s} = 0$, $P_{j,s}^{c} = 0$, and $I_{ij}^{sqr} \le \overline{I}_{ij}$; otherwise, $P_{j,s}^{c} = \Delta V \cdot \overline{I}_{ij}$.

According to [37], the linearization of the right side of Equation (14) is performed as indicated below:

$$P_{ij}^2 + Q_{ij}^2 = \sum_{y=1}^{Y} m_{ij,y}^{s} \cdot \Delta P_{ij,y} + \sum_{y=1}^{Y} m_{ij,y}^{s} \cdot \Delta Q_{ij,y};\ \ \forall ij \in \Omega_l \tag{31}$$

$$P_{ij}^{+} - P_{ij}^{-} = P_{ij};\ \ \forall ij \in \Omega_l \tag{32}$$

$$P_{ij}^{+} + P_{ij}^{-} = \sum_{y=1}^{Y} \Delta P_{ij,y};\ \ \forall ij \in \Omega_l \tag{33}$$

$$0 \le \Delta P_{ij,y} \le \overline{\triangle S}_{ij};\ \ \forall ij \in \Omega_l, \forall y \in 1..Y \tag{34}$$

$$Q_{ij}^{+} - Q_{ij}^{-} = Q_{ij};\ \ \forall ij \in \Omega_l \tag{35}$$

$$Q_{ij}^{+} + Q_{ij}^{-} = \sum_{y=1}^{Y} \Delta Q_{ij,y};\ \ \forall ij \in \Omega_l \tag{36}$$

$$0 \le \Delta Q_{ij,y} \le \overline{\triangle S}_{ij};\ \ \forall ij \in \Omega_l, \forall y \in 1..Y \tag{37}$$

$$0 \le P_{ij}^{+}, P_{ij}^{-}, Q_{ij}^{+}, Q_{ij}^{-};\ \ \forall ij \in \Omega_l \tag{38}$$

The right-hand side of constraint (31) is a linear approximation of the square active and reactive powers (P_{ij}^2, Q_{ij}^2). Constraints (32) and (35) represent the possible values for variables P_{ij} and Q_{ij} as a function of the auxiliary variables P_{ij}^{+}, P_{ij}^{-}, Q_{ij}^{+}, and Q_{ij}^{-}. Constraints (33) and (36) indicate that $|P_{ij}|$ and $|Q_{ij}|$ are the sum of the values in each

discretization block. Constraints (34) and (37) define the upper and lower limits of each block's contribution to $|P_{ij}|$ and $|Q_{ij}|$, respectively. Constraint (38) represents the non-negativity of auxiliary variables P_{ij}^{+}, P_{ij}^{-}, Q_{ij}^{+}, and Q_{ij}^{-}.

The following factors are taken into consideration when linearizing P_{ij}^{2} and Q_{ij}^{2}: the quantity of blocks of the piecewise linearization is Y; $m_{ij,y}^{s}$ indicates the slope of block y_{th} of the load flow at circuit ij; $\Delta P_{ij,y}$ and $\Delta Q_{ij,y}$ represent the values of the y_{th} block of $|P_{ij}|$ and $|Q_{ij}|$, respectively; $\overline{\Delta} S_{ij}$ is the maximum limit of every block of the load flow at branch ij; P_{ij}^{+} and P_{ij}^{-} are implemented to obtain $|P_{ij}|$; and Q_{ij}^{+} and Q_{ij}^{-} are used to obtain $|Q_{ij}|$. Equations (39) and (40) are used to calculate the values of $m_{ij,y}^{s}$, and $\overline{\Delta} S_{ij}$.

$$m_{ij,y}^{s} = (2y-1)\overline{\Delta} S_{ij} \tag{39}$$

$$\overline{\Delta} S_{ij} = \overline{V} \cdot \overline{I}_{ij} / Y \tag{40}$$

Equation (14) takes on the following form after the linearization shown above:

$$\left(\underline{V}^{2} + \frac{1}{2}\Delta V\right) I_{ij}^{sqr} + \sum_{s=1}^{S} P_{j,s}^{c} = \sum_{y=1}^{Y} m_{ij,y}^{s} \cdot \Delta P_{ij,y} + \sum_{y=1}^{Y} m_{ij,y}^{s} \cdot \Delta Q_{ij,y}; \forall ij \in \Omega_{l} \tag{41}$$

The linearization of the mathematical model of VR is given by Equations (42)–(53). Initially, Equation (9) is modified as indicated by Equation (42). Then, as the right side of Equation (42) is the product of two variables, it must be linearized as shown in Equations (43)–(45).

$$V_{j}^{sqr} = t_{ij}^{sqr} \cdot \widetilde{V}_{j}^{sqr};\ \forall ij \in \Omega_{l} \tag{42}$$

$$t_{ij}^{sqr} \cdot \widetilde{V}_{j}^{sqr} = t_{ij}^{sqr}\left(\underline{V}^{2} + \frac{1}{2}\Delta V\right) + \sum_{s=1}^{S} V_{j,s}^{c};\ \forall ij \in \Omega_{l} \tag{43}$$

$$(1-R\%)^{2}\Delta V\left(1-x_{j,s}\right) \leq t_{ij}^{sqr}\Delta V - V_{j,s}^{c} \leq (1+R\%)^{2}\Delta V\left(1-x_{j,s}\right);\ \forall ij \in \Omega_{b}; s = 1..S \tag{44}$$

$$(1-R\%)^{2}\Delta V \cdot x_{j,s} \leq V_{j,s}^{c} \leq (1+R\%)^{2}\Delta V \cdot x_{j,s};\ \forall ij \in \Omega_{b}; s = 1..S \tag{45}$$

The square voltage regulator tap, multiplied by the middle point of the first interval of the discretization of the square voltage magnitude, plus the subsequent voltage correction ($V_{j,s}^{c}$) that depends on ΔV, t_{ij}^{sqr} and $x_{j,s}$, is a linear approximation used to calculate the product $t_{ij}^{sqr} \cdot \widetilde{V}_{j}^{sqr}$. Equations (45) and (46) define the range of possible values that $V_{j,s}^{c}$ can take.

Variable t_{ij}^{sqr} in Equation (42) is squared; therefore, Equation (10) must be squared, as shown in Equation (46).

$$t_{ij,t}^{sqr} = 1 + 2R\%\left(\frac{nt_{ij}}{\overline{N}^{vr}}\right) + (R\%)^{2}\left(\frac{nt_{ij}}{\overline{N}^{vr}}\right)^{2};\ \forall\ ij \in \Omega_{l} \tag{46}$$

The last term in Equation (46), which is squared, varies between 0 and 1; therefore, according to [41], where the equal-area criterion is used, this term can be replaced by a constant of 1/3. Thus, Equation (46) takes the following form:

$$t_{ij,t}^{sqr} = 1 + 2R\%\left(\frac{nt_{ij}}{\overline{N}^{vr}}\right) + \frac{1}{3} \cdot (R\%)^{2};\ \forall\ ij \in \Omega_{l} \tag{47}$$

The position of a voltage regulator is indicated by using the binary variable W_{ij}^{vr} in Equation (11), as shown in (48).

$$-\overline{N}^{vr} \cdot W_{ij}^{vr} \leq nt_{ij} \leq \overline{N}^{vr} \cdot W_{ij}^{vr}; \ \ \forall\, ij \in \Omega_l \tag{48}$$

Equation (49) indicates the maximum number of VRs that may be installed in the PDS and Equations (50) and (51) define the type of variables used in the OPVR.

$$\sum_{\forall ij \in \Omega_l} W_{ij}^{vr} \leq \overline{N}_{syst}^{vr}; \ \ \forall\, ij \in \Omega_l \tag{49}$$

$$nt_{ij} \ \text{ integer}; \ \ \forall\, ij \in \Omega_l \tag{50}$$

$$W_{ij}^{vr} \in [0,1]; \ \ \forall\, ij \in \Omega_l \tag{51}$$

Finally, Equations (52) and (53) are used to calculate the regulated voltage and increase the precision of the presented model, as stated in [37].

$$\left| V_j^{sqr} - \widetilde{V}_j^{sqr} \right| \leq \left(\overline{V}^2 - \underline{V}^2 \right) W_{ij}^{vr}; \ \forall ij \in \Omega_l \tag{52}$$

$$\left| V_j^{sqr} - t_{ij}^{sqr} \left(\underline{V}^2 + \frac{1}{2} \Delta V \right) - \sum_{s=1}^{S} V_{j,s}^{c} \right| \leq \left(\overline{V}^2 - \underline{V}^2 \right) \left(1 - W_{ij}^{rt} \right); \forall ij \in \Omega_l \tag{53}$$

Equation (17) is modified as shown in (54) to consider the current limit in branches or VRs.

$$0 \leq I_{ij}^{sqr} \leq \overline{I}_{ij}^2 \left(y_{ij}^{+} + y_{ij}^{-} \right) \left(1 - W_{ij}^{rt} \right) + \min\{ \overline{I}_{vr}^2, \overline{I}_{ij}^2 \} \left(y_{ij}^{+} + y_{ij}^{-} \right) W_{ij}^{rt}; \ \ \forall ij \in \Omega_l \tag{54}$$

2.5. MILP Model for Optimal DNR and OPVR

The proposed MILP model for DNR and OPVR consists of minimizing active power losses and the installation cost of the VRs given by Equation (8). This objective function is subject to several constraints. Power balance constraints for active and reactive power are given by Equations (2) and (3); the voltage drop constraint, modified to consider the reconfiguration process, is given by Equation (13). The apparent power flow constraint given by Equation (5) is replaced by its linear equivalent given by Equation (41), the linearization procedure of the left- and right-hand sides of (5) is indicated by Equations (26)–(30) and (32)–(38), respectively. The voltage limit constraint is indicated in Equation (16), the constraints related to the DNR problem are given by (18)–(24), and finally, the constraint related to the output voltage of the VR is linearized using Equations (43)–(45), (47)–(53), and (54). To summarize, the proposed MILP model for optimal DNR and OPVR is provided below.

$$\text{Minimize} \ \ (8) \tag{55}$$

$$\begin{aligned} \text{Subject to:} \ \ & (2), (3), (13), (41), (26)\text{–}(30) \\ & (32)\text{–}(38), (16), (18)\text{–}(24), \\ & (43)\text{–}(45), (47)\text{–}(53), (54) \end{aligned} \tag{56}$$

3. Results

The optimal DNR and OPVRs proposed in this paper were modeled in AMPL and solved through CEPLEX using the default options. AMPL is a mathematical modeling language widely used in the scientific community for solving mathematical programming problems. It is an interface that reads the files in which the mathematical model is described and uses optimization solvers in charge of finding the solution to the model [42,43]. It is worth mentioning that the proposed model can be implemented in any other modeling language and using any other suitable MILP solver. The simulations were executed on a laptop with an Intel i7-8850H processor. Three different test systems were used to show the

performance of the proposed model. The data from the three test systems can be consulted in [44]. The following cases were considered for each test system:

- Case I: Initial Base case.
- Case II: Only DNR.
- Case III: Only OPVRs.
- Case IV: Simultaneous DNR and OPVRs.

For the sake of clarity, these hypotheses were considered:

1. The interest rate of the cost of active power losses (k_e) is assumed to be 168 USD/kW-year [45].
2. The cost of installation of each VR (C^{vr}) is 10,000 USD/line independently of its location in the distribution system [41].
3. The depreciation factor D is assumed as 10% [46,47].
4. The maximum number of VR ($\overline{N}^{vr}_{syst}$) is equal to 3 but can be set to any other limit.
5. To guarantee the quality of service supply, distribution network operators must maintain voltages within certain ranges. Admissible voltage magnitudes are between 0.90 to 1.05 p.u.
6. As the problem is approached from the distribution planning standpoint, the degradation of VRs due to commutation is neglected.

3.1. Results of the 33-Bus Test System

The 33-bus test system has 5 interconnection switches that are normally open, 32 normally closed switches, and 37 branches. In the initial case, switches 33 to 37 are open (see Figure 2). The nominal voltage of the test system is 12.66 kV, and there is a demand of $(3715 + j2300)$ kVA. The power loss for the initial case is 202.6771 kW. The system data are available in [44].

Table 1 presents the results of the proposed methodology considering the four explained cases. Note that in case I (initial base case), the minimum voltage is 0.9131 p.u., which is near the minimum allowed value of 0.9 p.u. In case II, when only DNR is considered, the open switches are 7,9, 14, 32, and 37. In this case, there is an important improvement in the voltage profile, with a minimum voltage magnitude of 0.9378 p.u. Note that there is also an important reduction in power losses; they pass from 202.67 (Case I) to 139.55 kW, which represents an improvement of 31.14% concerning the base case. Case III only considers the OPVRs without DNR. Note that the reduction in power losses is not as high as with reconfiguration and represents a relatively small reduction with respect to the base case (3.1%). This is because VRs do not inject power into the network. In Case IV, when both VRs and DNR are considered, the open switches are 7, 10, 14, 17, and 37. This solution is illustrated in Figure 3. In this case, there is both an important reduction in power losses and an improvement in voltage profile.

Figure 4 illustrates the bus voltages of the 33-bus test system considering the four cases under study. It can be seen that the combination of VRs and DNR results in the best voltage profile, while in the initial state, there are some buses close to the minimum allowable voltage limit of 0.9 p.u.

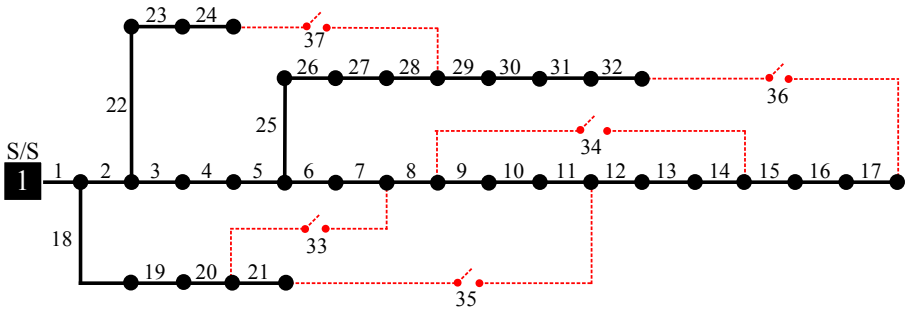

Figure 2. Initial topology of the 33-bus test system.

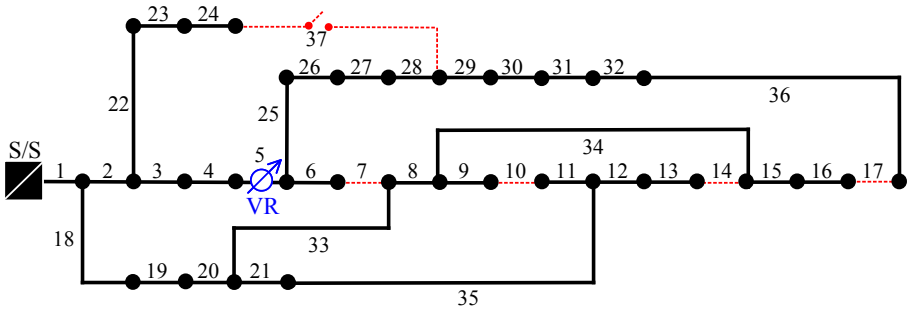

Figure 3. Optimal solution of the 33-bus test system for Case IV.

Table 1. Results of the 33-bus test system.

Case	Open Switches	Total Cost USD	VRs Cost USD	Losses Cost USD	Voltage Regulator		Power Losses (kW)	Vmin (p.u)	Time (s)
					Taps	Branch			
I	33 to 37	34,048	–	34,048	–	–	202.67	0.9131	–
II	7, 9, 14, 32, 37	23,744	–	23,444	–	–	139.55	0.9378	0.46
III	33 to 37	43,035	10,000	33,035	+8	6	196.64	0.9635	0.26
IV	7, 10, 14, 17, 37	36,550	10,000	26,550	+5	6	158.04	0.9606	25.18

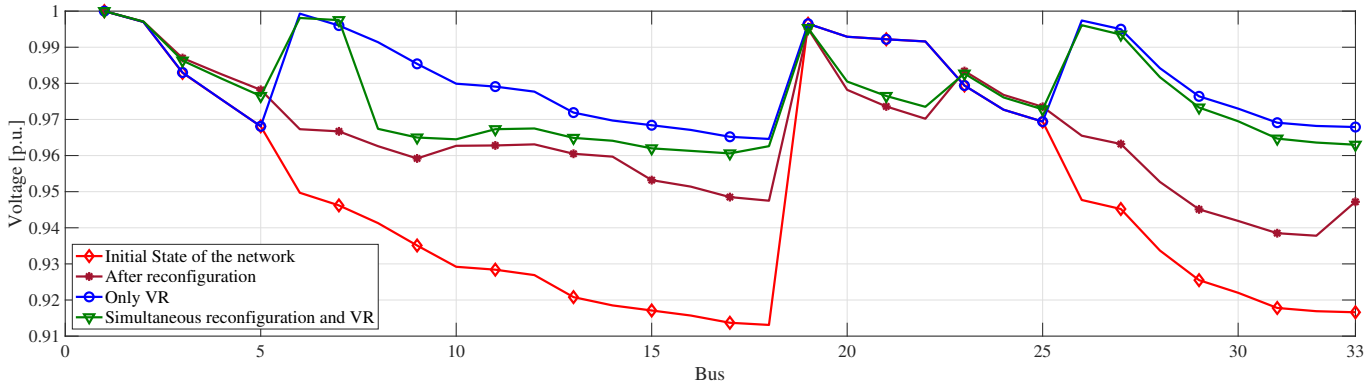

Figure 4. Voltage profile of the 33-bus test system.

3.2. Results of the 69-Bus Test System

The 69-bus test system, depicted in Figure 5, has 5 interconnection switches (normally open), 68 tie switches normally closed, and 73 branches. In the initial base case, switches 69 to 73 are open. This system has a nominal voltage of 12.66 kV with a demand of $(3802.19 + j2694.6)$ kVA. The data in this system can be consulted in [44].

The results of this test system based on the four cases under study are displayed in Table 2. The initial power losses amount to 224.99 kW, and the minimum voltage is 0.9092 p.u. After reconfiguration (case II), the open switches are 14, 55, 61, 69, and 70. In this case, power losses are 99.61 kW, which represents a reduction of 55.7% with respect to the base case. Furthermore, an important improvement in the voltage profile is achieved since the minimum voltage after reconfiguration is 0.9427 p.u. Case III considers OPVRs without reconfiguration. Therefore, the open switches of the base case remain the same. The proposed model only considers the installation of a single VR at bus 49. In this case, there is an important improvement in the voltage profile due to the effect of the VR. The minimum voltage is now 0.9564 p.u., representing an improvement of 5.19% compared to the initial base case. Power losses are 215.19 kW, representing a reduction of 4.4% concerning the base case. This small reduction in power losses is because VRs do not inject power into the network and are envisaged to improve the voltage profile and not reduce power losses. Case IV combines OPVRs with DNR. In the solution obtained with

the proposed model, switches 10, 13, 20, 56, and 61 are open (see Figure 6). In this case, there is a reduction of 51.9% in power losses with respect to the initial base case, and also the voltage profile is improved since the minimum voltage is 0.9534 p.u.

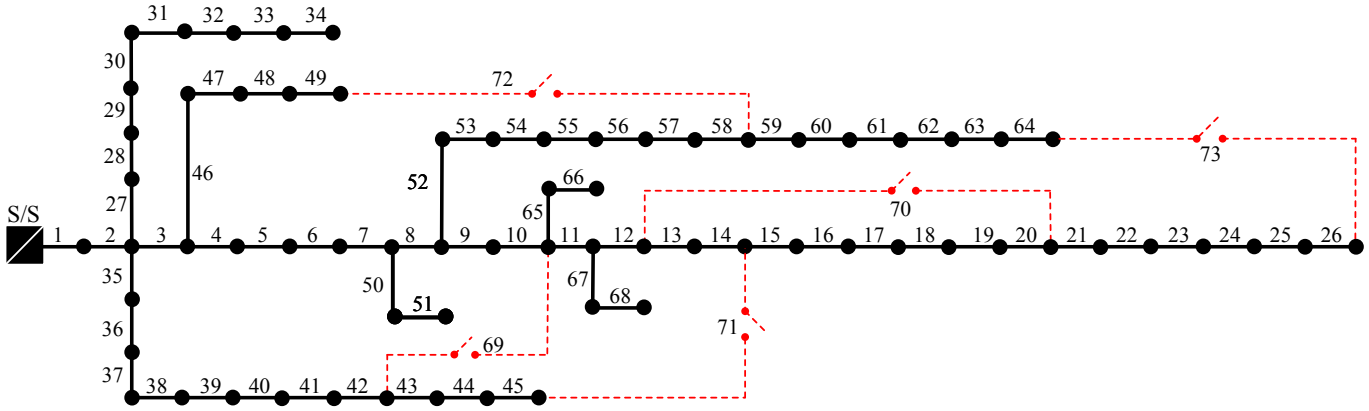

Figure 5. Initial topology of the 69-bus test system.

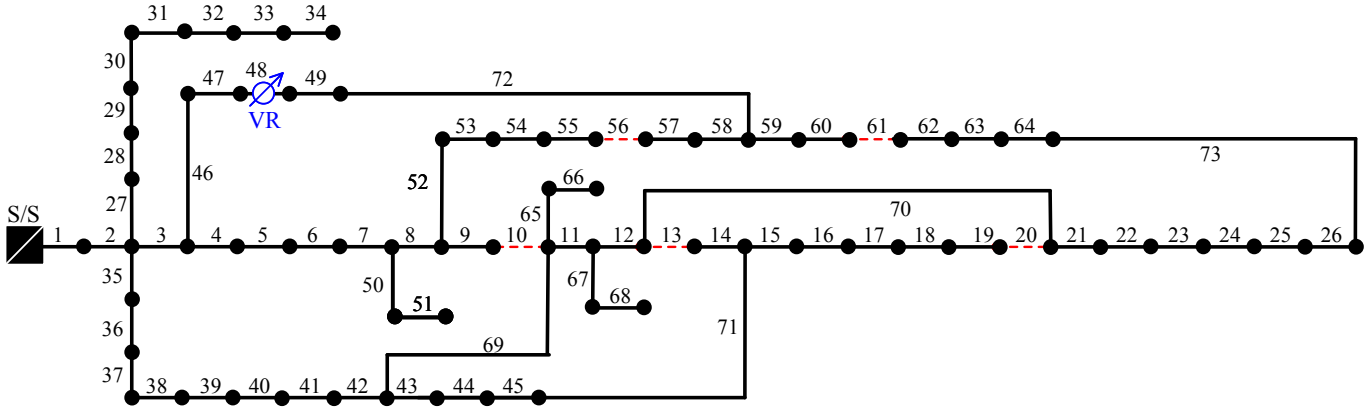

Figure 6. Optimal solution of the 69-bus test system.

Table 2. Results of the 69-bus test system.

Case	Open Switches	Total Cost USD	VRs Cost USD	Losses Cost USD	Voltage Regulator		Power Losses (kW)	Vmin (p.u)	Time (s)
					Taps	Branch			
I	69 to 73	37,798	–	37,798	–	–	224.99	0.9092	–
II	14, 55, 61, 69, 70	16,734	–	16,734	–	–	99.61	0.9427	2.42
III	69 to 73	46,120	10,000	36,120	+7	57	215.01	0.9564	0.38
IV	10, 13, 20, 56, 61	28,179	10,000	18,179	+1	49	108.18	0.9551	83.78

Figure 7 depicts the nodal voltages of the 69-bus test system considering the four cases under study. Note that the inclusion of the VR and the optimal reconfiguration improves the voltage profile of the system.

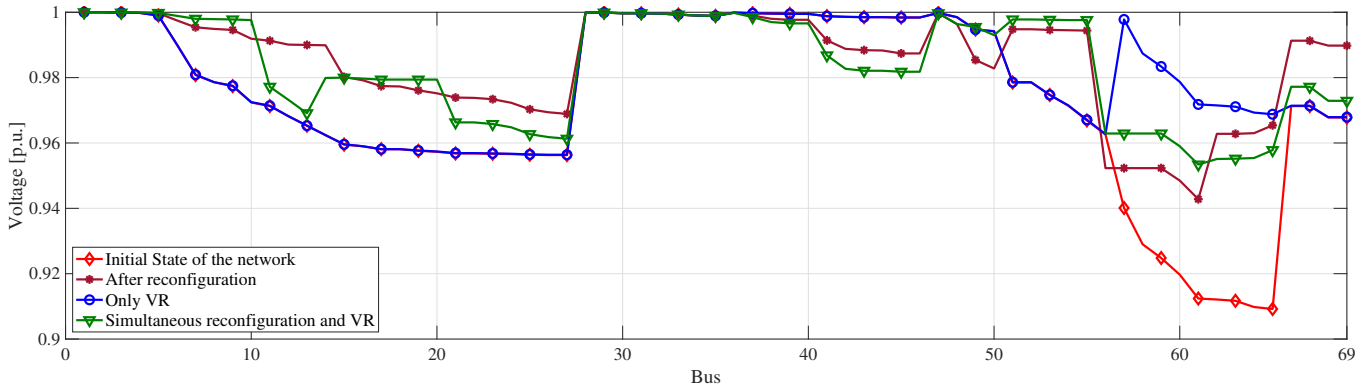

Figure 7. Voltage profile of the 69-bus test system.

3.3. Results of the 119-Bus Test System

This test system has 133 branches, 15 interconnection switches, and 118 tie switches (see Figure 8). Initially, switches 119, 120, 121, 122, 123, 124, 125, 126, 127, 128, 129, 130, 131, 132, and 133 are open. This system has a nominal voltage of 11.0 kV and a total demand of (22,709.72 + *j*17,041.067) kVA. In the initial base case, the active power losses are 1296.57 kW. The data of this system can be consulted in [44].

The results for the 119-bus test system for the cases under consideration are presented in Table 3. Note that in the base case (case I), the minimum voltage is 0.8687 p.u. This represents a critical value that is not accepted by most distribution operators since it is below 0.9 p.u.

After reconfiguration (Case II), the open switches are 24, 26, 35, 40, 43, 51, 59, 72, 75, 96, 98, 11, 122, 130, and 131. In this case, power losses are 853.58 kW, which represents a reduction of 34.16% with respect to the initial base case. Further, the minimum voltage after reconfiguration is 0.9322 p.u., representing an important improvement with respect to the initial state of the network. In Case III, the proposed model only considers the installation of a single VR at bus 121 (end bus), which corresponds to branch 116, resulting in a minimum voltage of 0.9053, which represents an important improvement with respect to the base case. Nonetheless, the reduction in power losses is not very important. As already mentioned, this is because VRs do not inject power into the network. Case IV combines OPVRs with DNR. In the solution obtained with the proposed model, switches 23, 26, 35, 39, 43, 51, 59, 72, 75, 96, 98, 110, 122, 130, and 131 are open (see Figure 9). Note that there is not only an important reduction in power losses but also an improvement in voltage profile. In this case, power losses are 874.59 kW, and the minimum voltage is 0.9501 p.u. This demonstrates that for this system, the combination of VR and DNR results in an attractive solution for system planers, not only from the standpoint of power loss reduction but also from the standpoint of voltage profile improvement.

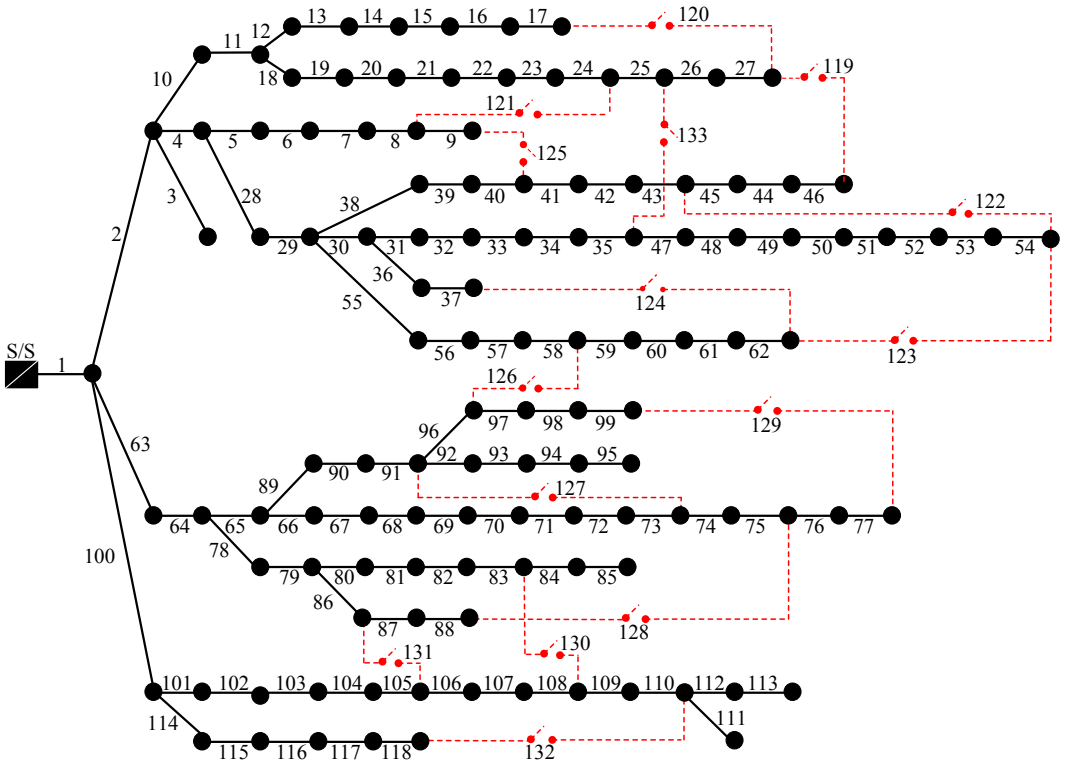

Figure 8. Initial topology of the 119-bus test system.

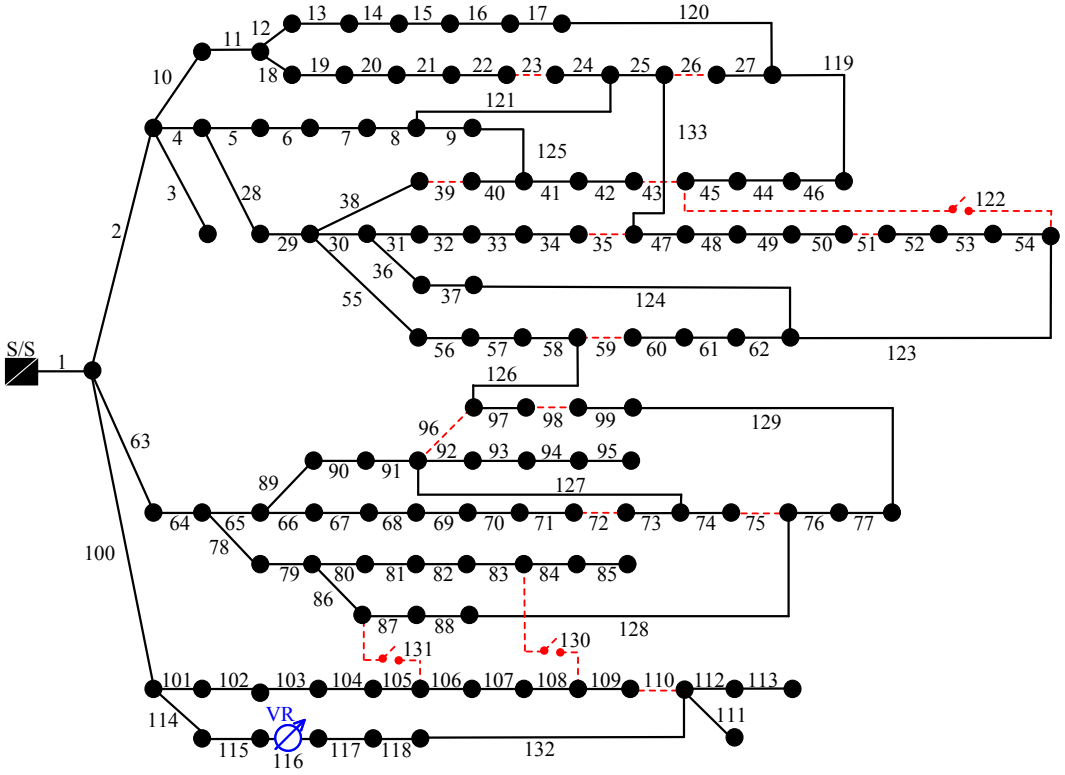

Figure 9. Optimal solution of the 119-bus test system.

Table 3. Results of the 119-bus test system.

Case	Open Switches	Total Cost USD	VRs Cost USD	Losses Cost USD	Voltage Regulator		Power Losses (kW)	Vmin (p.u)	Time (s)
					Taps	Branch			
I	119 to 133	217,823	–	217,823	–	–	1296.57	0.8687	–
II	24, 26, 35, 40, 43, 51, 59, 72, 75, 96, 98, 110, 122, 130, 131	143,401	–	143,401	–	–	853.58	0.9322	10.73
III	135 to 156	224,996	10,000	214,996	+13	71	1279.74	0.9053	3.48
IV	23, 26, 35, 39, 43, 51, 59, 72, 75, 96, 98, 110, 122, 130, 131	156,931	10,000	146,931	+7	121	874.59	0.9501	1,136.10

Figure 10 depicts the nodal voltages of the 119-bus test system. It should be noted that four buses are below the acceptable minimum voltage of 0.9 p.u. in the initial base case; however, as reconfiguration and the VR are installed in the network, the voltage profile significantly improves, ensuring that all voltage buses are within acceptable limits.

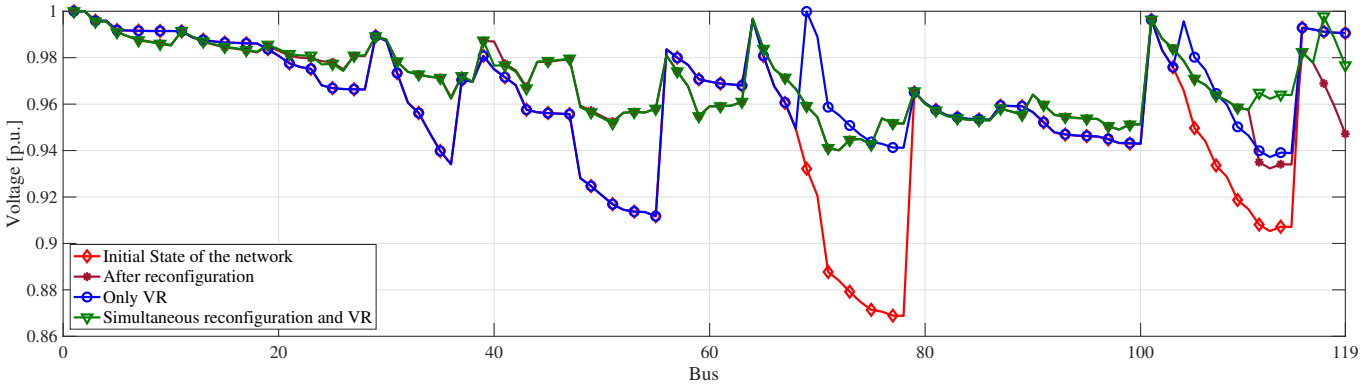

Figure 10. Voltage profile of the 119-bus test system.

4. Comparative Analysis of Results

This section presents a comparative analysis of the proposed approach with previous research works reported in the specialized literature. Furthermore, an analysis of the effect of DG units in the model is also presented. The comparative analysis was carried out with the 33 and 69-bus test systems. while the analysis of the effect of DG was considered with the 119-bus test system. In this latter case, the location and sizing of the DG units are considered parameters instead of optimization variables.

4.1. Comparison with Other Research Works

To the best of the author's knowledge, the simultaneous DNR and OPVRs have not been approached in the specialized literature. As a result, the comparative analysis was limited to works that only involved DNR or OPVRs. For the 33-bus test system, when the optimal reconfiguration was carried out alone, the same results as those reported in [48–52] were found. As regards the optimal allocation of VRs, Table 4 shows a comparative analysis of the reported results for the optimal placement of VRs in the 33-bus test system.

In [21], the optimal placement of VRs is carried out through DPSO (Discrete Particle Swarm Optimization). In this case, three VRs are proposed to be installed at buses 4, 5, and 6, obtaining power losses of 3.99% and the maximum voltage regulation of 4.55%. Although this solution reports the lowest power losses, its main drawback lies in the high investment cost since three VRs are installed instead of only one, as found with the proposed approach (MILP). Furthermore, better voltage regulation is obtained in both solutions found by the implemented MILP models.

Table 4. Comparative results for the 33-bus test system.

Method	VR at Bus	Power Loss (%)	Voltage Regulation (%)
DPSO [21]	4, 5 and 6	3.99	4.53
DPSO [25,27]	5 and 6	4.15	2.86
PGSA [25,27]	5 and 6	4.09	2.85
MILP for OPVR	6	5.29	3.65
MILP for OPVR and DNR	6	4.25	3.94

In [25,27], the authors carry out the optimal allocation of VRs through DPSO and PGSA (Plant Growth Simulation Algorithm). For the 33-bus test system, five VRs are allocated from bus 2 to bus 6. Nonetheless, the VRs allocated at buses 2, 3, and 4 have their tap settings at 0, which means that they are not needed. The power losses reported for this solution are 4.15% and 4.09%, respectively.

In contrast with the aforementioned papers, our approach only considers one VR allocated at bus 6. The power losses obtained for the OPVR and OPVR with DNR are 5.29% and 4.25%, respectively. Note that although power losses are higher, the investment cost is significantly lower since only one VR is required. Furthermore, the regulation in both cases is better than the one reported in [21] but slightly higher than that reported in [25,27]. In this sense, the solution found by the proposed MILP approach for OPVRs and DNR is better since it involves more than one objective, so the power losses and voltage profile are optimized, and it requires lower investment (one VR instead of two).

For the 69-bus test system, the solution found for the reconfiguration alone is the same as the one reported in [49,51,53,54]. As regards OPVRs, Table 5 shows a comparative analysis of reported results in the 69-bus test system.

Table 5. Comparative results for the 69-bus test system.

Method	VR at Bus	Power Loss (%)	Voltage Regulation (%)
DPSO [21]	57 and 60	4.10	4.42
BT [24]	57	5.33	4.35
FL [24]	6 and 57	5.23	2.94
DPSO [25]	58, 59 and 60	4.15	4.98
PGSA [25]	57 and 60	4.09	4.13
BT [28]	57	5.34	4.35
MILP for OPVR	57	5.65	4.36
MILP for OPVR and DNR	49	2.84	4.49

It can be observed in Table 5 that the solution found by the proposed MILP model for simultaneous OPVRs and optimal DNR presents the lowest power losses (2.84%) with only one VR. In terms of investment costs, the solution found for the simultaneous OPVRs and optimal DNR is better than the ones reported in [21,24] (for fuzzy logic (FL) algorithm) [25] (for both DPSO and PGSA), and [28] since only one VR is required instead of two or three.

When applying the proposed model for only OPVRs, just one VR is placed (four of six consulted references use two VRs instead of one), and it is located on bus 57, which is consistent with the solutions reported in [24,28]. When comparing voltage regulation and power losses, it can be seen that voltage regulation is practically the same, and power losses present a difference of 5.8%.

4.2. Effect of DG in the Proposed Model

The presence of DG is ever-growing in modern EDNs. The reconfiguration problem considering the effect of DG has been approached in several studies [55–60]. Nonetheless, none of these research works consider the optimal placement and setting of VRs along with DNR and the optimal location and sizing of DG. In this sense, it is worth mentioning that the optimal allocation and sizing of DG within the DNR problem, including the optimal placement and setting of VRs, is a challenging optimization problem that is out of the scope of this research. Nonetheless, the presence of DG can be included in the model as fixed generators that provide energy to the network at a given power factor. For the sake of simplicity and without loss of generality, only the effect of DG on the 119-bus test system is analyzed. In this case, it is supposed that there are four DG units of 1000 kW, each operating at a lagging power factor of 0.9, located at buses 29, 52, 77, and 107.

The results of this new scenario are illustrated in Table 6. In this case, the open switches are 23, 26, 35, 40, 43, 52, 59, 71, 74, 83, 96, 98, 110, 122, and 131. The optimization process proposes the installation of a single VR at branch 117. The active power losses are 812.39 kW, representing a reduction of 37.34% with respect to the initial base case, and the minimum voltage is 0.9508 p.u. The introduction of DG units in the system results in a net reduction in the network demand, which brings lower power losses and an improved voltage profile (with respect to the base case). This solution is of similar quality to the one found for Case IV presented in Table 3; nonetheless, the installation cost of the DG units was not considered, which allows the conclusion that the cost would be significantly higher than the one reported in Table 6.

Table 6. Results of the 119-bus test system considering DG.

Open Switches	Total Cost USD	VRs Cost USD	Losses Cost USD	Voltage Regulator		Power Losses (kW)	Vmin (p.u)	Time (s)
				Taps	Branch			
23, 26, 35, 40, 43, 52, 59, 71, 74, 83, 96, 98, 110, 122, 131	146,481	10,000	136,481	+1	117	812.39	0.9508	1294.10

5. Conclusions

Distribution network reconfiguration, along with optimal placement and setting of voltage regulators, play an important role in modern distribution systems since their combined effects allow for reducing power losses and improving voltage profile. This paper presented a MILP model that allows solving the optimal DNR and OPVRs either separately or jointly, the latter being the first time reported in the specialized literature.

To show the applicability and effectiveness of the proposed approach, several tests were carried out in three benchmark distribution systems of 33, 69, and 119 buses. For the optimal DNR alone, the proposed model found the same results previously reported in the specialized literature. As regards OPVRs alone, for the 33-bus test system, the proposed model was able to find a better solution than the one reported in the literature, requiring a single VR. This contrasts with previously reported solutions that consider two VRs, implying higher investment costs.

For the 69-bus test system, the proposed model was able to find the same location of the VR as reported in other papers, obtaining similar results regarding power losses and voltage regulation. Further, better results were presented when contrasted with other research works that proposed two or three VRs for this system, implying higher investment costs. Furthermore, for the 119-bus test system, the optimal location of VRs is reported for the first time in the literature, which can be used as a reference for further research on the subject.

The results allow for the conclusion that the optimal placement and setting of VRs has an important effect concerning the improvement of voltage profile; however, it presents a relatively low impact on power losses. This is due to the fact that VRs do not inject power into the network. Nonetheless, the combined effect with DNR is able to find solutions with

both low power losses and a high voltage profile. This is especially useful in distribution networks with long feeders, loaded circuits, and a poor voltage profile.

The versatility of the proposed model was tested by including the effect of DG in the 119-bus test system. As expected, the presence of this type of generation results in lower active power losses and improved voltage profile; nonetheless, the installation of DG might result in higher costs to the network. In this sense, the optimal location and sizing of DG units within the DNR and OPVRs are proposed as a topic of future research.

Finally, the solutions for the combined optimal DNR and OPVRs are reported for the first time in the literature for 33, 69, and 119-bus test systems. These data can be used by other researchers for comparative purposes in further studies.

Author Contributions: Conceptualization, L.G.P., J.L.-L. and O.G.C.; Data curation, L.G.P., J.L.-L. and O.G.C.; Formal analysis, L.G.P., J.L.-L. and O.G.C.; Funding acquisition, L.G.P., J.L.-L. and O.G.C.; Investigation, L.G.P., J.L.-L. and O.G.C.; Methodology, L.G.P., J.L.-L. and O.G.C.; Project administration, L.G.P., J.L.-L. and O.G.C.; Resources, L.G.P., J.L.-L. and O.G.C.; Software, L.G.P., J.L.-L. and O.G.C.; Supervision, L.G.P., J.L.-L. and O.G.C.; Validation, L.G.P., J.L.-L. and O.G.C.; Visualization, L.G.P. and O.G.C.; Writing—original draft, L.G.P.; Writing—review & editing, L.G.P. All authors have read and agreed to the published version of the manuscript.

Funding: This research received no external funding.

Institutional Review Board Statement: Not applicable.

Informed Consent Statement: Not applicable.

Data Availability Statement: Not applicable.

Acknowledgments: The authors would like to thank the Colombia Scientific Program within the framework of the so-called Ecosistema Científico (Contract No. FP44842- 218-2018).

Conflicts of Interest: The authors declare that they have no conflict of interest.

References

1. Rullo, P.G.; Braccia, L.; Feroldi, D.; Zumoffen, D. Multivariable Control Structure Design for Voltage Regulation in Active Distribution Networks. *IEEE Lat. Am. Trans.* **2022**, *20*, 839–847. [CrossRef]
2. Razavi, S.M.; Momeni, H.R.; Haghifam, M.R.; Bolouki, S. Multi-Objective Optimization of Distribution Networks via Daily Reconfiguration. *IEEE Trans. Power Deliv.* **2022**, *37*, 775–785. [CrossRef]
3. Gallego Pareja, L.A.; López-Lezama, J.M.; Gómez Carmona, O. A Mixed-Integer Linear Programming Model for the Simultaneous Optimal Distribution Network Reconfiguration and Optimal Placement of Distributed Generation. *Energies* **2022**, *15*, 3063. [CrossRef]
4. López-Lezama, J.M.; Cortina-Gómez, J.; Munoz, N. Assessment of the Electric Grid Interdiction Problem using a nonlinear modeling approach. *Electr. Power Syst. Res.* **2017**, *144*, 243–254. [CrossRef]
5. Montoya, O.D.; Grisales-Noreña, L.F.; Perea-Moreno, A.J. Optimal Investments in PV Sources for Grid-Connected Distribution Networks: An Application of the Discrete-Continuous Genetic Algorithm. *Sustainability* **2021**, *13*, 13633. [CrossRef]
6. Jaramillo Serna, J.d.J.; López-Lezama, J.M. Alternative Methodology to Calculate the Directional Characteristic Settings of Directional Overcurrent Relays in Transmission and Distribution Networks. *Energies* **2019**, *12*, 3779. [CrossRef]
7. Li, Y.; Hao, G.; Liu, Y.; Yu, Y.; Ni, Z.; Zhao, Y. Many-Objective Distribution Network Reconfiguration Via Deep Reinforcement Learning Assisted Optimization Algorithm. *IEEE Trans. Power Deliv.* **2022**, *37*, 2230–2244. [CrossRef]
8. Saldarriaga-Zuluaga, S.D.; López-Lezama, J.M.; Muñoz-Galeano, N. Adaptive protection coordination scheme in microgrids using directional over-current relays with non-standard characteristics. *Heliyon* **2021**, *7*, e06665. [CrossRef]
9. Montoya, O.D.; Gil-González, W.; Grisales-Noreña, L.F. Solar Photovoltaic Integration in Monopolar DC Networks via the GNDO Algorithm. *Algorithms* **2022**, *15*, 277. [CrossRef]
10. Agudelo, L.; López-Lezama, J.M.; Muñoz-Galeano, N. Vulnerability assessment of power systems to intentional attacks using a specialized genetic algorithm. *Dyna* **2015**, *82*, 78–84. [CrossRef]
11. Eldurssi, A.M.; O'Connell, R.M. A Fast Nondominated Sorting Guided Genetic Algorithm for Multi-Objective Power Distribution System Reconfiguration Problem. *IEEE Trans. Power Syst.* **2015**, *30*, 593–601. [CrossRef]
12. Zhang, J.; Yuan, X.; Yuan, Y. A novel genetic algorithm based on all spanning trees of undirected graph for distribution network reconfiguration. *J. Mod. Power Syst. Clean Energy* **2014**, *2*, 143–149. [CrossRef]
13. Srinivasa Rao, R.; Narasimham, S.V.L.; Ramalinga Raju, M.; Srinivasa Rao, A. Optimal Network Reconfiguration of Large-Scale Distribution System Using Harmony Search Algorithm. *IEEE Trans. Power Syst.* **2011**, *26*, 1080–1088. [CrossRef]

14. dos Santos, M.V.; Brigatto, G.A.; Garcés, L.P. Methodology of solution for the distribution network reconfiguration problem based on improved harmony search algorithm. *IET Gener. Transm. Distrib.* **2020**, *14*, 6526–6533. [CrossRef]
15. Dias Santos, J.; Marques, F.; Garcés Negrete, L.P.; Andrêa Brigatto, G.A.; López-Lezama, J.M.; Muñoz-Galeano, N. A Novel Solution Method for the Distribution Network Reconfiguration Problem Based on a Search Mechanism Enhancement of the Improved Harmony Search Algorithm. *Energies* **2022**, *15*, 2083. [CrossRef]
16. Shetty, V.J.; Ankaliki, S.G. Electrical Distribution System Power Loss Reduction and Voltage Profile Enhancement by Network Reconfiguration Using PSO. In Proceedings of the 2019 Fifth International Conference on Electrical Energy Systems (ICEES), Chennai, India, 21–22 February 2019; pp. 1–4. [CrossRef]
17. Kumar, B.; Saw, B.K.; Bohre, A.K. Optimal Distribution Network Reconfiguration to Improve the System Performances using PSO with Multiple-Objectives. In Proceedings of the 2020 International Conference on Computational Intelligence for Smart Power System and Sustainable Energy (CISPSSE), Keonjhar, India, 29–31 July 2020; pp. 1–6. [CrossRef]
18. Pegado, R.; Ñaupari, Z.; Molina, Y.; Castillo Correa, C. Radial distribution network reconfiguration for power losses reduction based on improved selective BPSO. *Electr. Power Syst. Res.* **2019**, *169*, 206–213. [CrossRef]
19. Mahdavi, M.; Alhelou, H.H.; Bagheri, A.; Djokic, S.Z.; Ramos, R.A.V. A Comprehensive Review of Metaheuristic Methods for the Reconfiguration of Electric Power Distribution Systems and Comparison With a Novel Approach Based on Efficient Genetic Algorithm. *IEEE Access* **2021**, *9*, 122872–122906. [CrossRef]
20. Safigianni, A.; Salis, G. Optimum voltage regulator placement in a radial power distribution network. *Power Syst. IEEE Trans.* **2000**, *15*, 879–886. [CrossRef]
21. Rao, J.; Sivanagaraju, S. Voltage Regulator Placement in Radial Distribution System Using Discrete Particle Swarm Optimization. *Int. Rev. Electr. Eng.* **2008**, *3*, 525–531.
22. Ganesh Vulasala, S.n.S.; Thiruveedula, R. Genetic algorithm based voltage regulator placement in unbalanced radial distribution systems. *Acta Electroteh.* **2009**, *50*, 253–259.
23. Pereira, C.; Castro, C. Optimal placement of voltage regulators in distribution systems. In Proceedings of the 2009 IEEE Bucharest PowerTech, Bucharest, Romania, 28 June–2 July 2009; pp. 1–5. [CrossRef]
24. Visali. Nagalamadaka, S.S.; Sankar, V. Loss Reduction in Radial Distribution Systems by Optimal Voltage Regulator Placement Using Fuzzy Logic. *Int. J. Electr. Eng.* **2010**, *3*, 147–160.
25. Rao, P.R.; Raju, S.S. Voltage regulator placement in radial distribution system using plant growth simulation algorithm. *Int. J. Eng. Sci. Technol.* **2010**, *2*, 207–217. [CrossRef]
26. Mendoza Baeza, J.; Peña, H. Automatic voltage regulators siting in distribution systems considering hourly demand. *Lancet* **2011**, *81*, 1124–1131. [CrossRef]
27. Manikandan, S.; Sasitharan, S.; Rao, J.V. Analysis of Optimal AVR Placement in Radial Distribution Systems using Discrete Particle Swarm Optimization. *Innov. Syst. Des. Eng.* **2012**, *3*, 27–42.
28. Salkuti Surender Reddy, L.Y.H. Optimum location of voltage regulators in the radial distribution systems. *Int. J. Emerg. Electr. Power Syst.* **2016**, *17*, 351–361. [CrossRef]
29. Pimentel Filho, M.C.; Medeiros, M. Localization of voltage regulators in distribution systems by a mixed Genetic–Tabu search algorithm. *Energy Power Eng.* **2013**, *5*, 751–755. [CrossRef]
30. Attar, M.; Homaee, O.; Falaghi, H.; Siano, P. A novel strategy for optimal placement of locally controlled voltage regulators in traditional distribution systems. *Int. J. Electr. Power Energy Syst.* **2018**, *96*, 11–22. [CrossRef]
31. Muthukumar, K.; Jayalalitha, S.; Sureshkumar, K.; Sakthivel, A. Artificial Bee Colony Algorithm Based Placement and Optimal Tap Selection of Voltage Regulators for Power Loss Minimization in Distribution System. *Int. J. Pure Appl. Math.* **2018**, *118*, 2295–2313.
32. Molla Addisu, A.O.S.; Takele, H. Fuzzy logic based optimal placement of voltage regulators and capacitors for distribution systems efficiency improvement. *Heliyon* **2021**, *7*, e07848. . [CrossRef]
33. Shaheen, A.M.; El-Sehiemy, R.A. Optimal Coordinated Allocation of Distributed Generation Units/ Capacitor Banks/ Voltage Regulators by EGWA. *IEEE Syst. J.* **2021**, *15*, 257–264. [CrossRef]
34. Gallego, L.A.; López-Lezama, J.M.; Gómez, O. Optimal Placement of Capacitors, Voltage Regulators, and Distributed Generators in Electric Power Distribution Systems. *Ingeniería* **2020**, *25*, 334–354. [CrossRef]
35. Zhou, A.; Zhai, H.; Yang, M.; Lin, Y. Three-Phase Unbalanced Distribution Network Dynamic Reconfiguration: A Distributionally Robust Approach. *IEEE Trans. Smart Grid* **2022**, *13*, 2063–2074. [CrossRef]
36. Navesi, R.B.; Nazarpour, D.; Ghanizadeh, R.; Alemi, P. Switchable Capacitor Bank Coordination and Dynamic Network Reconfiguration for Improving Operation of Distribution Network Integrated with Renewable Energy Resources. *J. Mod. Power Syst. Clean Energy* **2022**, *10*, 637–646. [CrossRef]
37. Franco, J.F.; Rider, M.J.; Lavorato, M.; Romero, R. A mixed-integer LP model for the optimal allocation of voltage regulators and capacitors in radial distribution systems. *Int. J. Electr. Power Energy Syst.* **2013**, *48*, 123–130. [CrossRef]
38. Gallego, L.A.; Franco, J.F.; Cordero, L.G. A fast-specialized point estimate method for the probabilistic optimal power flow in distribution systems with renewable distributed generation. *Int. J. Electr. Power Energy Syst.* **2021**, *131*, 107049. [CrossRef]
39. Cespedes, R.G. New method for the analysis of distribution networks. *IEEE Trans. Power Deliv.* **1990**, *5*, 391–396. [CrossRef]
40. Gallego, L.A.; López-Lezama, J.M.; Carmona, O.G. A Mixed-Integer Linear Programming Model for Simultaneous Optimal Reconfiguration and Optimal Placement of Capacitor Banks in Distribution Networks. *IEEE Access* **2022**, *10*, 52655–52673. [CrossRef]

41. Franco, J.; Lavorato, M.; Rider, M.J.; Romero, R. An efficient implementation of tabu search in feeder reconfiguration of distribution systems. In Proceedings of the 2012 IEEE Power and Energy Society General Meeting, San Diego, CA, USA, 22–26 July 2012; pp. 1–8. [CrossRef]
42. Olszak, A.; Karbowski, A. Parampl: A Simple Tool for Parallel and Distributed Execution of AMPL Programs. *IEEE Access* **2018**, *6*, 49282–49291. [CrossRef]
43. Gay, D.M. The AMPL Modeling Language: An Aid to Formulating and Solving Optimization Problems. *Numer. Anal. Optim.* **2015**, *134*, 95–116. [CrossRef]
44. Gallego, L.A.; López-Lezama, J.M.; Gómez, O. Data of the Electrical Distribution Systems for the Optimal Reconfiguration Used in This Paper, 2022. Available online: https://github.com/LuisGallego2019/ElectricalSystemsDataForReconfiguration (accessed on 15 October 2022).
45. Ramesh Babu, M.; Kumar, C.; Anitha, S. Simultaneous Reconfiguration and Optimal Capacitor Placement Using Adaptive Whale Optimization Algorithm for Radial Distribution System. *J. Electr. Eng. Technol.* **2020**, *16*, 181–190. [CrossRef]
46. Gnanasekaran, N.; Chandramohan, S.; Kumar, P.S.; Mohamed Imran, A. Optimal placement of capacitors in radial distribution system using shark smell optimization algorithm. *Ain Shams Eng. J.* **2016**, *7*, 907–916. [CrossRef]
47. Salimon, S.; Suuti, K.; Adeleke, H.; Ebenezer, O.K.; Aderinko, H. Impact of Optimal Placement and Sizing of Capacitors on Radial Distribution Network using Cuckoo Search Algorithm. *Curr. J. Appl. Sci. Technol.* **2020**, *15*, 39–49. [CrossRef]
48. Lavorato, M.; Franco, J.F.; Rider, M.J.; Romero, R. Imposing Radiality Constraints in Distribution System Optimization Problems. *IEEE Trans. Power Syst.* **2012**, *27*, 172–180. [CrossRef]
49. Abdelaziz, A.; Mohamed, F.; Mekhamer, S.; Badr, M. Distribution system reconfiguration using a modified Tabu Search algorithm. *Electr. Power Syst. Res.* **2010**, *80*, 943–953. [CrossRef]
50. Hijazi, H.; Thiébaux, S. Optimal distribution systems reconfiguration for radial and meshed grids. *Int. J. Electr. Power Energy Syst.* **2015**, *72*, 136–143.
51. Mahdavi, M.; Alhelou, H.H.; Hatziargyriou, N.D.; Al-Hinai, A. An Efficient Mathematical Model for Distribution System Reconfiguration Using AMPL. *IEEE Access* **2021**, *9*, 79961–79993. [CrossRef]
52. Taylor, J.A.; Hover, F.S. Convex Models of Distribution System Reconfiguration. *IEEE Trans. Power Syst.* **2012**, *27*, 1407–1413. [CrossRef]
53. Khorshid-Ghazani, B.; Seyedi, H.; Mohammadi-ivatloo, B.; Zare, K.; Shargh, S. Reconfiguration of distribution networks considering coordination of the protective devices. *IET Gener. Transm. Distrib.* **2017**, *11*, 82–92. [CrossRef]
54. Abdelaziz, A.; Mohammed, F.; Mekhamer, S.; Badr, M. Distribution Systems Reconfiguration using a modified particle swarm optimization algorithm. *Electr. Power Syst. Res.* **2009**, *79*, 1521–1530. [CrossRef]
55. Quadri, I.; Bhowmick, S. A hybrid technique for simultaneous network reconfiguration and optimal placement of distributed generation resources. *Soft Comput.* **2020**, *24*. [CrossRef]
56. Siahbalaee, J.; Rezanejad, N.; Gharehpetian, G.B. Reconfiguration and DG Sizing and Placement Using Improved Shuffled Frog Leaping Algorithm. *Electr. Power Components Syst.* **2019**, *47*, 1475–1488.
57. Ben Hamida, I.; Salah, S.; Faouzi, M.; Mimouni, M. Optimal integration of distributed generations with network reconfiguration using a Pareto algorithm. *Int. J. Renew. Energy Res.* **2018**, *8*, 345–356.
58. Chen, Q.; Wang, W.; Wang, H.; Wu, J.; Wang, J. An Improved Beetle Swarm Algorithm Based on Social Learning for a Game Model of Multiobjective Distribution Network Reconfiguration. *IEEE Access* **2020**, *8*, 200932–200952. [CrossRef]
59. Wang, C.; Lei, S.; Ju, P.; Chen, C.; Peng, C.; Hou, Y. MDP-Based Distribution Network Reconfiguration With Renewable Distributed Generation: Approximate Dynamic Programming Approach. *IEEE Trans. Smart Grid* **2020**, *11*, 3620–3631. [CrossRef]
60. Shojaei, F.; Rastegar, M.; Dabbaghjamanesh, M. Simultaneous placement of tie-lines and distributed generations to optimize distribution system post-outage operations and minimize energy losses. *CSEE J. Power Energy Syst.* **2021**, *7*, 318–328. [CrossRef]